Supplementary Figure 1

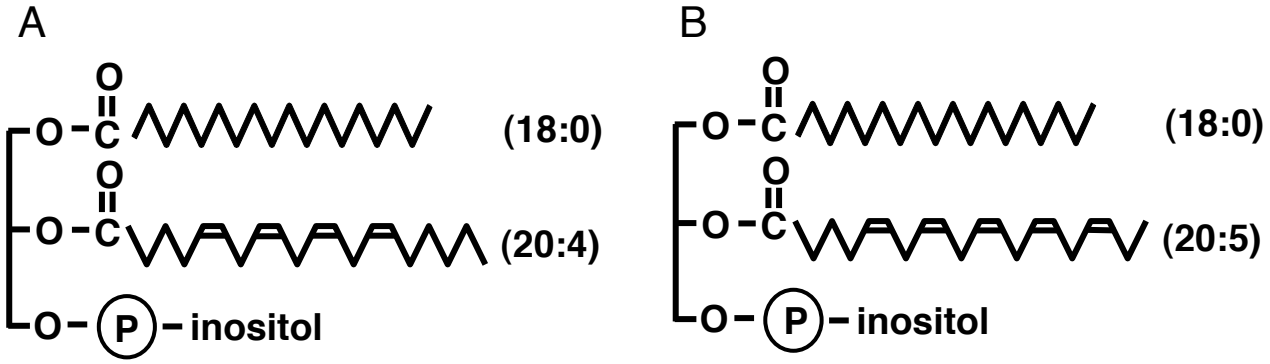

Supplementary Figure 1. The major molecular species of PI in mammals (A) and *C. elegans* (B).

Supplementary Figure 2

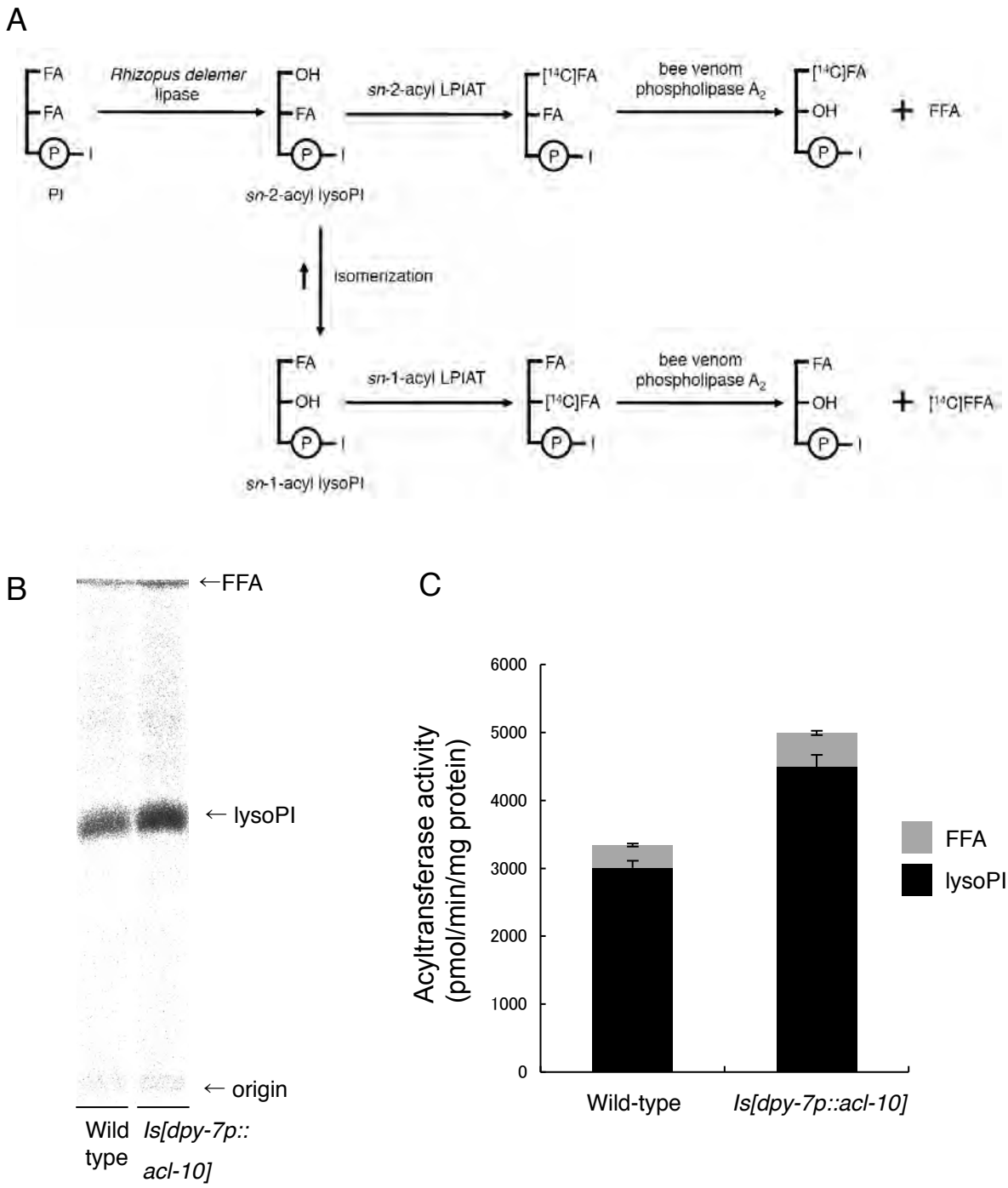

Supplementary Figure 2. A procedure for determining *sn*-2-acyl LPIAT activity. A scheme of the procedure is shown in (A). After the *in vitro* acyltransferase assay, the lipids were extracted and separated by TLC as described in *Materials and Methods*. The resulting PI fractions were re-extracted from the TLC plates and treated with phospholipase A_2. The distribution of radioactivity among the reaction products (free fatty acid and lysoPI) was assessed following TLC (B, C). Radiolabeled free fatty acid and lysoPI were indicated as gray bars and black bars, respectively (C). [^{14}C]stearoyl-CoA was used as an acyl donor. The membrane fraction of transgenic worms expressing ACL-10 showed increased stearoyl-CoA:*sn*-2-acyl LPIAT activity (C, compare black bars). "I", "FA" and "FFA" in panel A indicate inositol, fatty acid, and free fatty acid, respectively.

Supplementary Table 1 *C .elegans* AGPAT family

Gene	Sequence name	Human homologue
acl-1	F59F4.4	AGPAT1, AGPAT2
acl-2	T06E8.1	AGPAT1, AGPAT2
acl-3	ZK809.2	Tafazzin
acl-4	F49H12.6	GPAT3, GPAT4
acl-5	R07E3.5	GPAT3, GPAT4
acl-6	F08F3.2	GPAT1, GPAT2
acl-7	Y46G5A.21	DHAPAT
acl-8	T05H4.1	LYCAT
acl-9	ZK40.1	LYCAT
acl-10	F55A11.5	LYCAT
acl-11	F28B3.9	AGPAT5
acl-12	C01C10.3	LPGAT1
acl-13	F08G5.2	LPGAT1
acl-14	K07B1.5	LPGAT1

Supplementary Figure 3

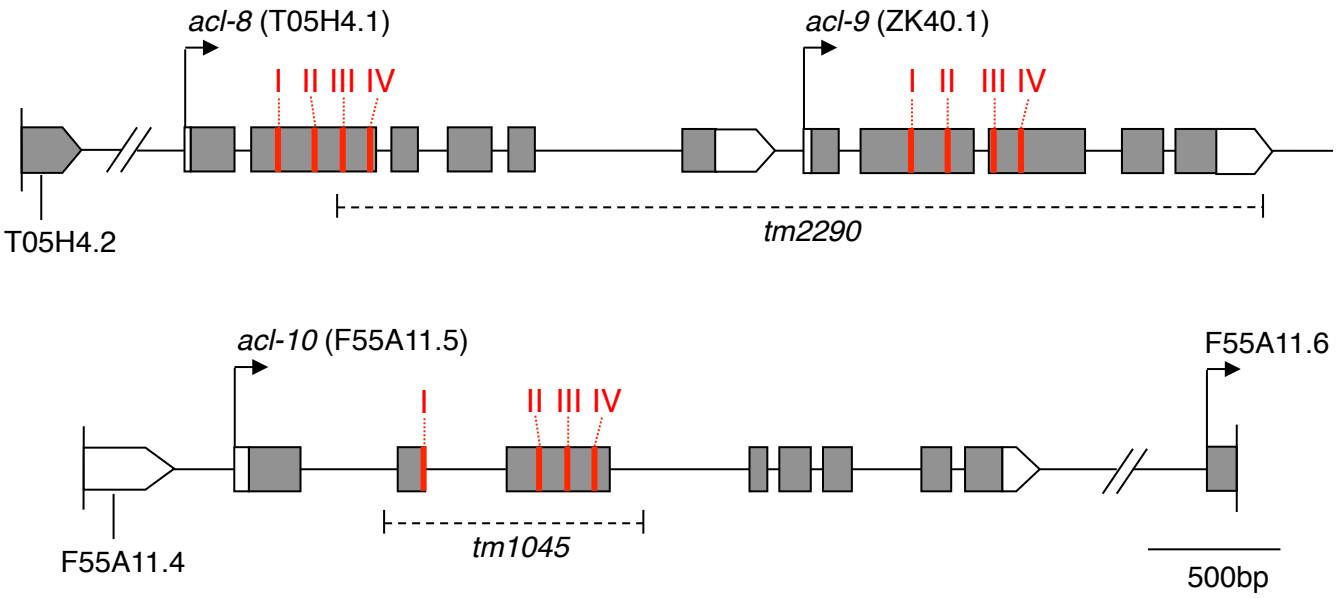

Supplementary Figure 3. Genomic structures of *acl-8, acl-9* and *acl-10*. The *acl-8, acl-9* and *acl-10* genes are located on chromosomes V. *acl-8* and *acl-9* are adjacent to each other. Gray and white boxes correspond to coding exons and UTRs, resepctively. The positions of the predicted conserved lysophospholipid acyltransferase motifs (motif I~IV), (Lewin *et al.*, 1999; Beigneux *et al.*, 2006), characteristic of AGPAT family members, are shown in red. The *tm2290* allele lacks the acyltransferase motif III and IV of *acl-8* and the entire *acl-9* genomic region, suggesting that this mutation is null allele of both *acl-8* and *acl-9*. The *tm1045* allele lacks all acyltransferase motifs of *acl-10*.

Supplementary Figure 4

A

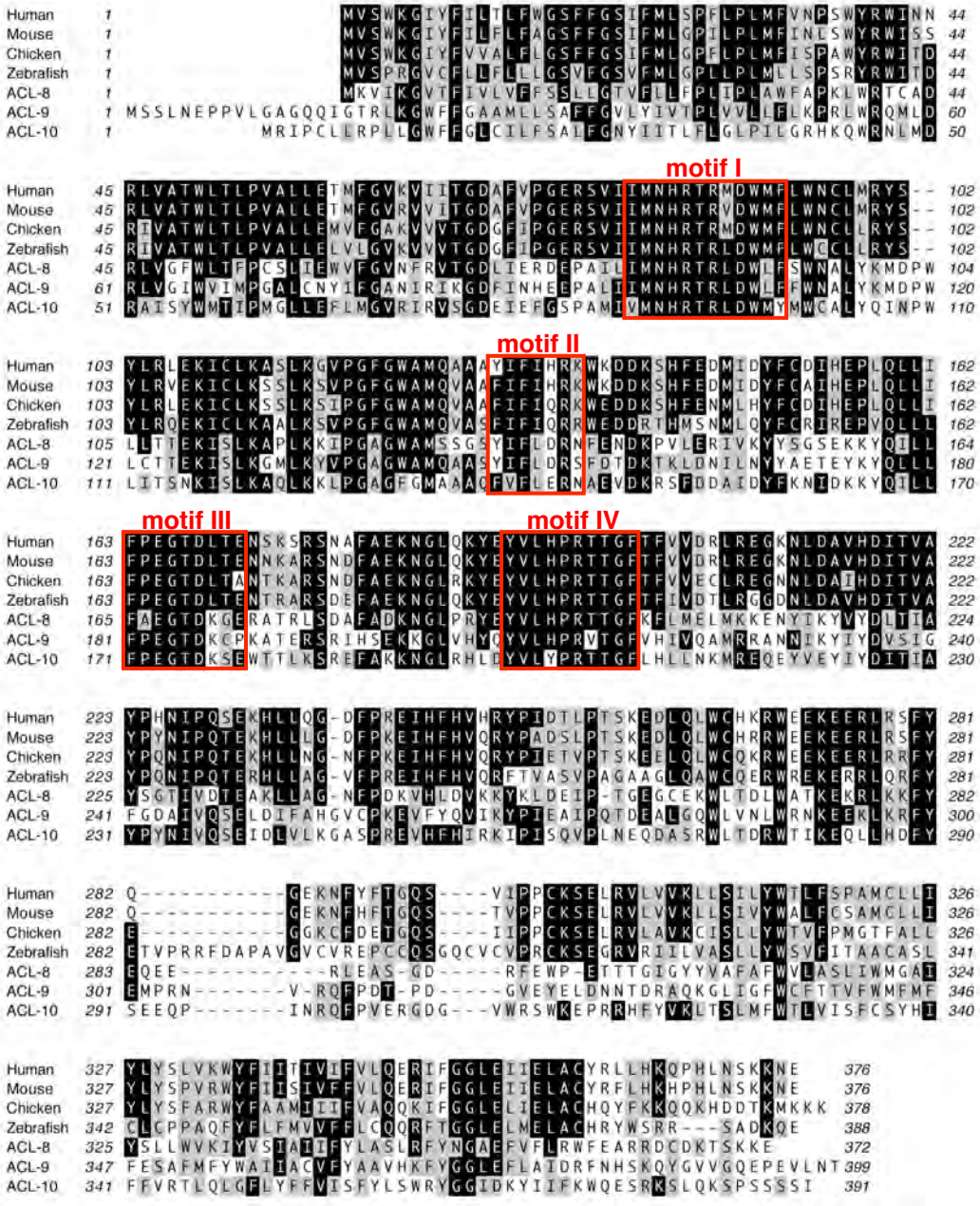

B

	motif I	motif II	motif III	motif IV
Human GPAT1	^{227}LPVHRSHIDYLL	^{273}GFFIRRR	^{313}FLEGTRSRS	^{347}ILIIPVGISY
Human AGPAT1	^{101}VSNHQSSLDLLG	^{144}VIFIDRK	^{176}FPEGTRNHN	^{203}VPIVPIVMSS
Human LYCAT	^{82}IMNHRTRMDWMF	^{130}YIFIHRK	^{163}FPEGTDLTE	^{191}YVLHPRTTGF
Mouse LYCAT	^{82}IMNHRTRVDWMF	^{130}FIFIHRK	^{163}FPEGTDLTE	^{191}YVLHPRTTGF
Chicken LYCAT	^{82}IMNHRTRMDWMF	^{130}FIFIQRK	^{163}FPEGTDLTA	^{191}YVLHPRTTGF
Zebrafish LYCAT	^{82}IMNHRTRLDWMF	^{130}FIFIQRR	^{163}FPEGTDLTE	^{191}YVLHPRTTGF
ACL-8	^{82}IMNHRTRLDWLF	^{132}YIFLDRN	^{165}FAEGTDKGE	^{193}YVLHPRTTGF
ACL-9	^{98}IMNHRTRLDWLF	^{148}YIFLDRS	^{181}FPEGTDKCP	^{209}YVLHPRVTGF
ACL-10	^{88}VMNHRTRLDWMY	^{138}FVFLERN	^{171}FPEGTDKSE	^{200}YVLYPRTTGF

Supplementary Figure 4. *acl-8*, *acl-9*, *acl-10* subfamily members in *C. elegans* are evolutionarily conserved. (A) Alignment of ACL-8, ACL-9, ACL-10 and their homologues (LYCAT) from human, mouse, chicken and zebrafish. Identical amino acids are shown on a black background and similar amino acids are on a grey background. The lysophospholipid acyltransferase motifs conserved in AGPAT family members are boxed. Accession numbers for the sequences used were as follows: human: NP_001002257; mouse: NP_001074540; chicken: NP_001026210; zebrafish: NP_998435; ACL-9: NP_504644; ACL-10: NP_505971. The amino acid sequence of ACL-8 was obtained from the sequence of *acl-8* cDNA clone (yk569g12.5, kindly provided by Y. Kohara) and was different from that in the Wormbase database (http://www.wormbase.org/). The deduced ACL-8 amino acid sequence is: MKVIKGVTFIVLVFFSSLLGTVFLLFPLIPLAWFAPKLWRTCADRLVGF WLTFPCSLIEWVFGVNFRVTGDLIERDEPAILIMNHRTRLDWLFSWNALYKMDPWLLTTEKISLKAPLK KIPGAGWAMSSGSYIFLDRNFENDKPVLERIVKYYSGSEKKYQILLFAEGTDKGERATRLSDAFADKN GLPRYEYVLHPRTTGFKFLMELMKKENYIKYVYDLTIAYSGTIVDTEAKLLAGNFPDKVHLDVKKYK LDEIPTGEGCEKWLTDLWATKEKRLKKFYEQEERLEASGDRFEWPETTTGIGYYVAFAFWVLASLIWM GAIYSLLWVKIYVSIAIIFYLASLRFYNGAEFVFLRWFEARRDCDKTSKKE. (B) Comparison of amino acid sequences of motif I~IV. Numbers refer to amino acid residue position within each protein sequence. Red amino acids show consensus motifs that define AGPAT family. Blue amino acids are highly conserved in LYCAT proteins of various species, but not conserved in other AGPAT family members. Most of these "LYCAT signature amino acids" are conserved in *C. elegans* ACL-8, ACL-9 and ACL-10. Accession number. : human GPAT1; AAH30783, human AGPAT1; NP_006402.

Supplementary Figure 5

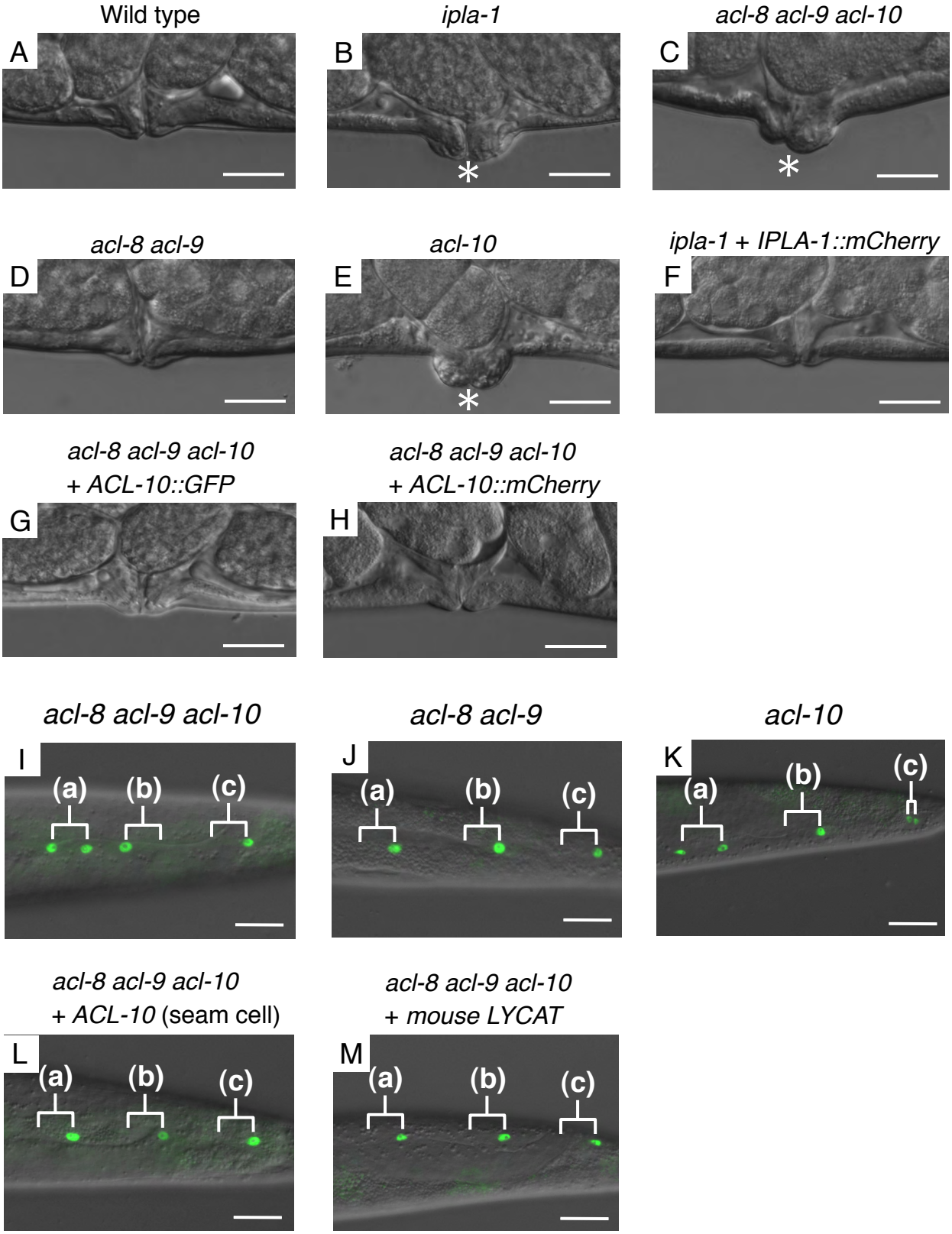

Supplementary Figure 5. Defects of vulval morphology and asymmetric cell division in *ipla-1* mutants, *acl-8 acl-9 acl-10* triple mutants and *acl-10* single mutants. (A-H) Vulval morphology. The protruding vulva phenotype (asterisk) observed in *ipla-1* mutants (B), *acl-8 acl-9 acl-10* mutants (C) and *acl-10* single mutants (E). Note that *acl-8 acl-9* double mutants show no defects in vulval morphology (D). The *dpy-7p::ipla-1::gfp* transgene fully rescue the vulval defects of *ipla-1* mutants (F). Both *acl-10p::acl-10::gfp* and *acl-10p::acl-10::mCherry* transgenes fully rescue the vulval defects of *acl-8 acl-9 acl-10* mutants (G, H). (I-M) Seam cells at the late L4 stage visualized by *scm::gfp*. Merged fluorescence and differential interference contrast images are shown. The letters (a), (b) and (c) correspond to those of Figure 3A. The asymmetry of the divisions is disrupted in *acl-8 acl-9 acl-10* mutants (I) and *acl-10* mutants (K), whereas it is normal in *acl-8 acl-9* double mutants (J). The expression of *acl-10* under the seam cell-specific *scm* promoter restores the normal asymmetric divisions in *acl-8 acl-9 acl-10* mutants (L), indicating that *acl-10* cell-autonomously acts in seam cells. The expression of mouse LYCAT restores the normal asymmetric divisions in *acl-8 acl-9 acl-10* mutants (M), indicating that mouse LYCAT is a functional orthologue of *C. elegans acl-8*, *acl-9*, *acl-10* subfamily members. Scale bars are 20 μm.

Supplementary Figure 6

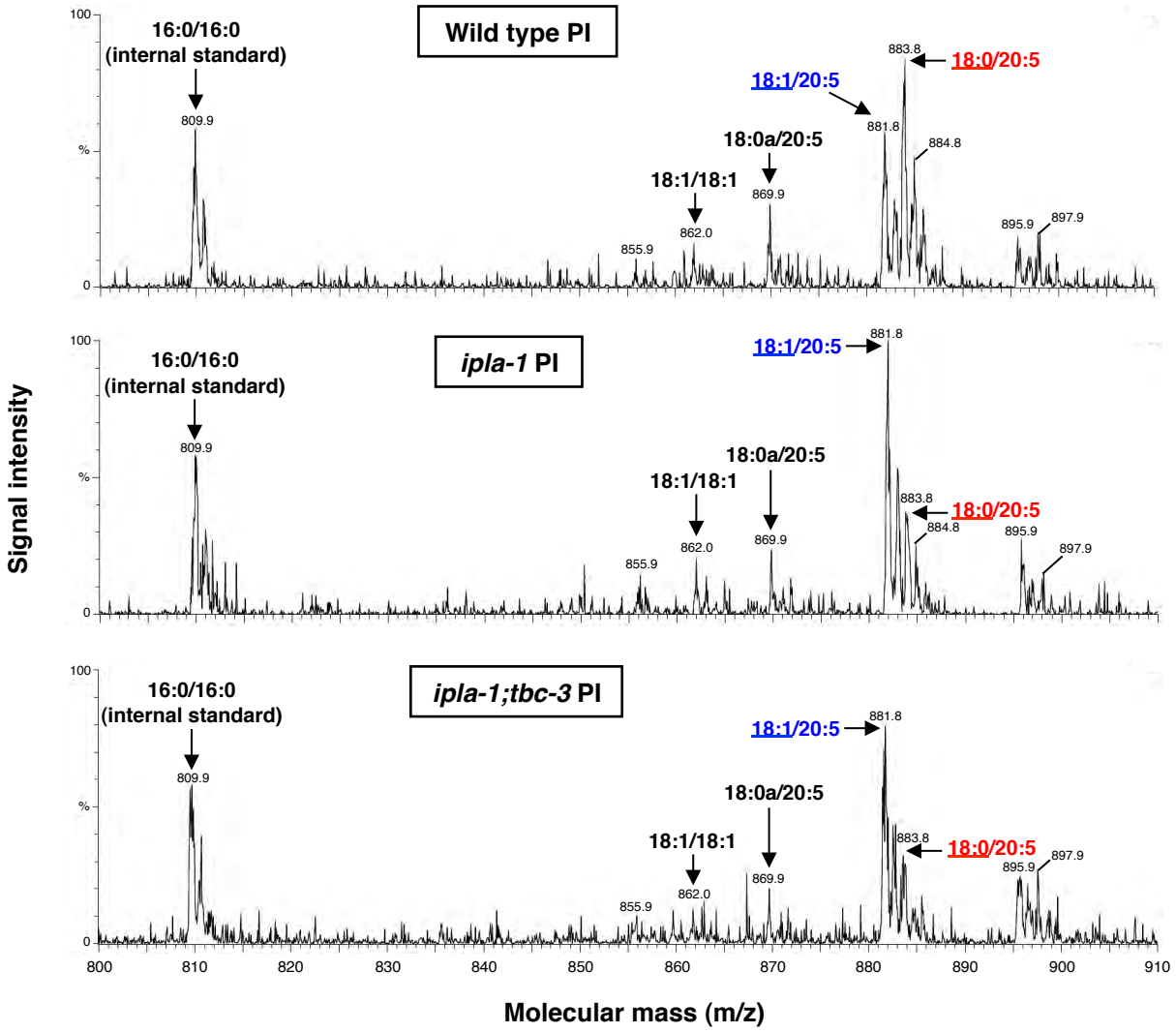

Supplementary Figure 6. Negative ionization LC/ESI-MS spectra of PI molecular species of wild-type (upper), *ipla-1* mutants (middle) and *ipla-1;tbc-3* double mutants (lower). 'a' refers to alkyl ether linkage.

Supplementary Figure 7

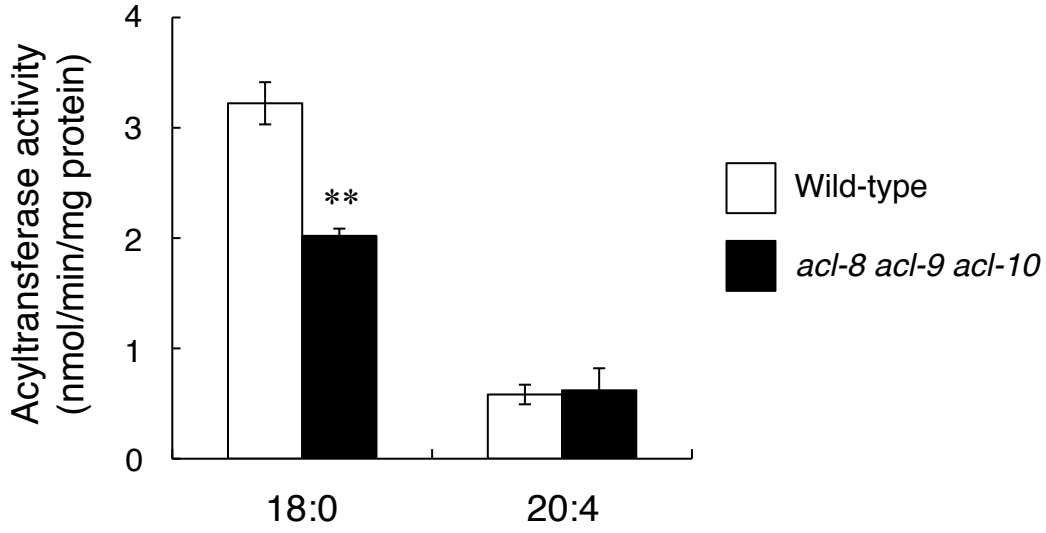

Supplementary Figure 7. *sn*-2-acyl LPIAT activities of wild-type and *acl-8 acl-9 acl-10* mutants were measured using [^{14}C]stearoyl-CoA (18:0-CoA) or [^{14}C]arachidonoyl-CoA (20:4n-6-CoA) as acyl donors. Each bar represents the mean ± SEM of at least three independent experiments. ***P*<0.01.

Supplementary Figure 8

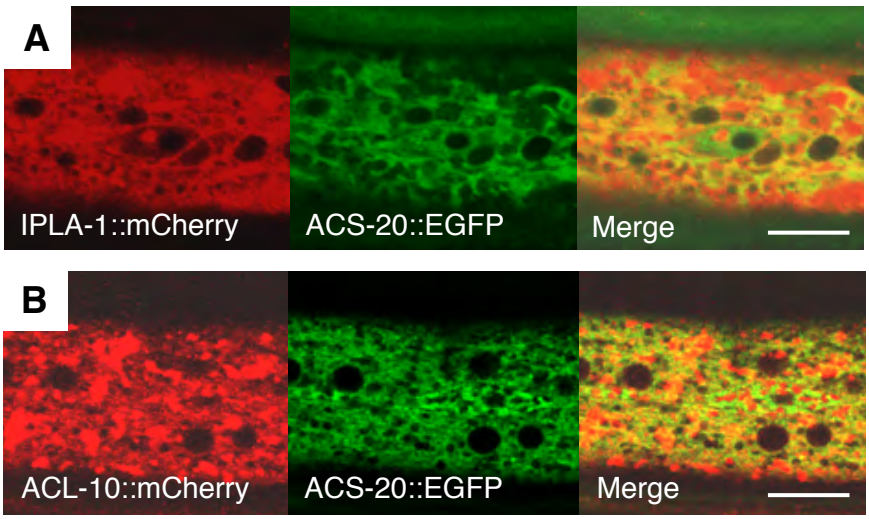

Supplementary Figure 8. Intracellular localizations of IPLA-1 and ACL-10
Confocal images of transgenic worms expressing IPLA-1::mCherry and the ER marker ACS-20::EGFP (A) and ACL-10::mCherry and ACS-20::EGFP (B). Full genotypes of these strains are *acs-20;acs-22;xhEx3526[dpy-7p::ipla-1::mCherry];tmEx1920[acs-20p::acs-20::egfp]* (A) and *acs-20;acs-22;xhEx3529[acl-10p::acl-10::mCherry];tmEx1920[acs-20p::acs-20::egfp]* (B). The *acl-10p::acl-10::mCherry* transgene also rescued the phenotypes of *acl-8 acl-9 acl-10* mutants (Supplementary Figure 4H), indicating that this fusion protein is functional.

Supplementary Figure 9

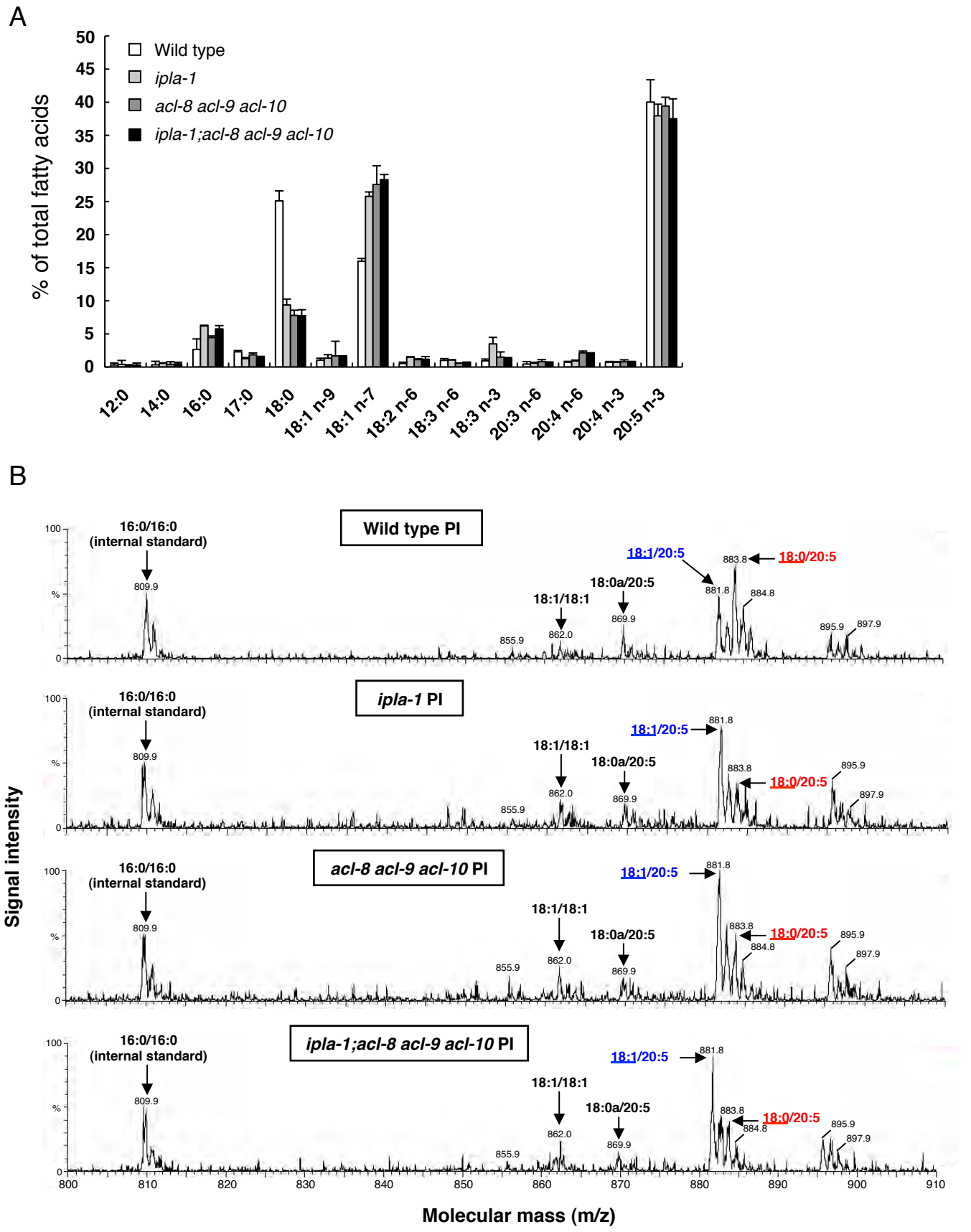

Supplementary Figure 9. Fatty acid composition of PI in *ipla-1; acl-8 acl-9 acl-10* quadruple mutants is similar to that in *ipla-1* mutants and *acl-8 acl-9 acl-10* mutants. (A) GC analysis of PI. Each bar represents the mean ± SEM of at least three independent experiments. (B) Negative ionization LC/ESI-MS spectra of PI molecular species. 'a' refers to alkyl ether linkage.

Supplementary Figure 10

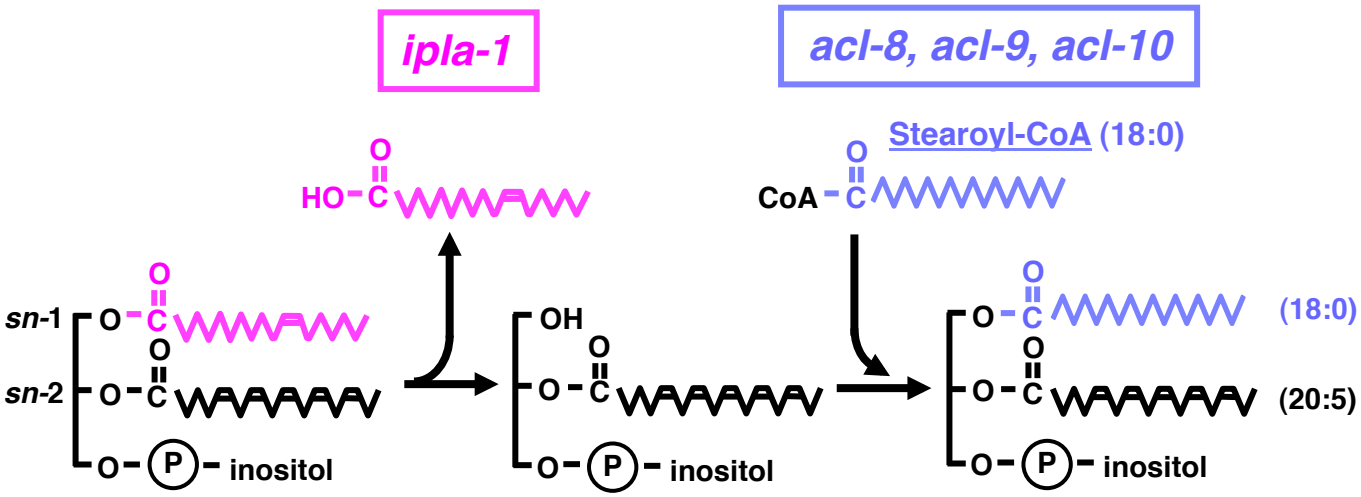

Supplementary Figure 10. Proposed model for determination of the *sn*-1 fatty acid composition of PI. *ipla-1* and *acl-8*, *-9*, *-10* subfamily members are the phospholipase A_1 and acyltransferases, respectively, which are involved in fatty acid remodeling of the *sn*-1 position of PI.

Supplementary Figure 11

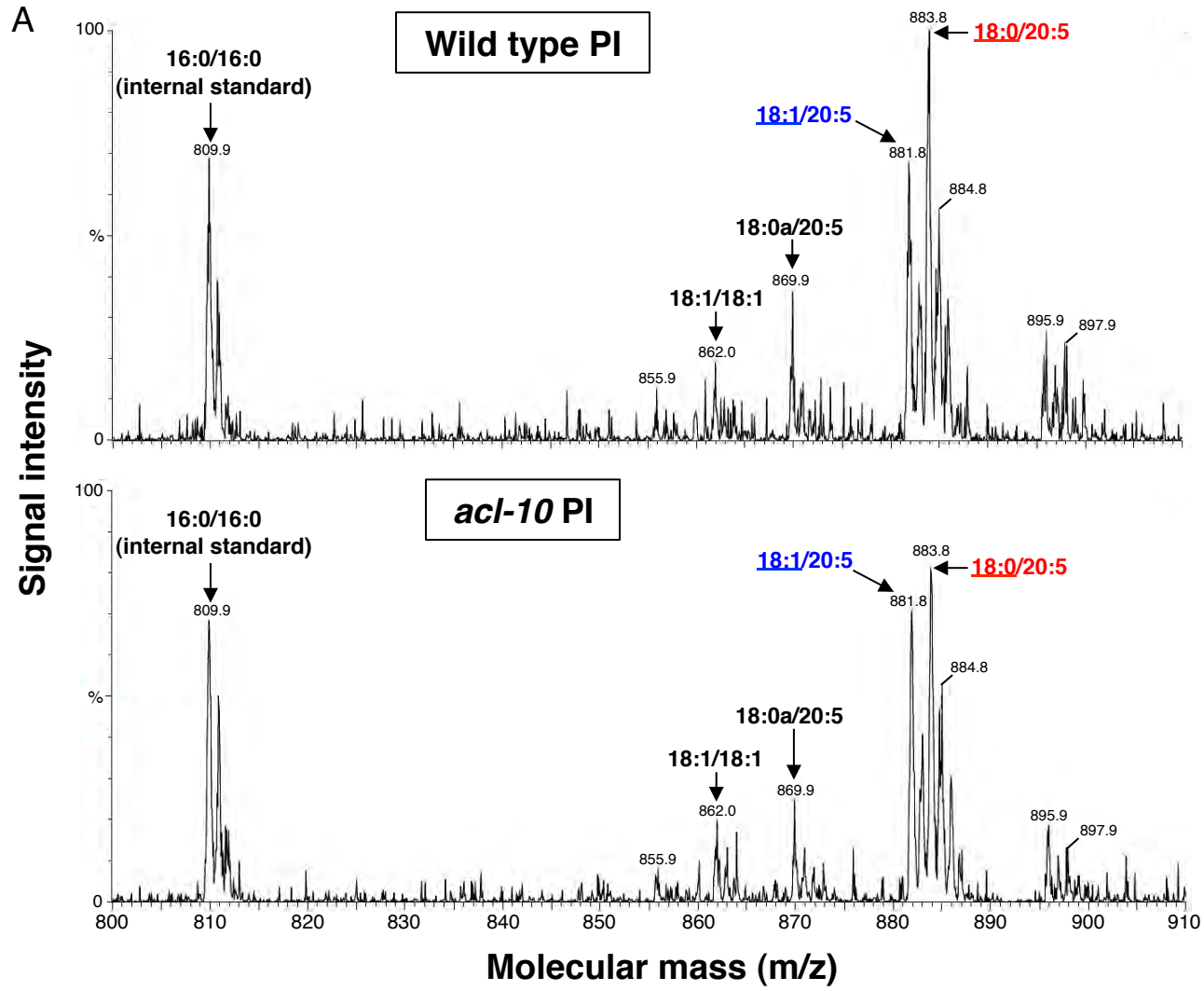

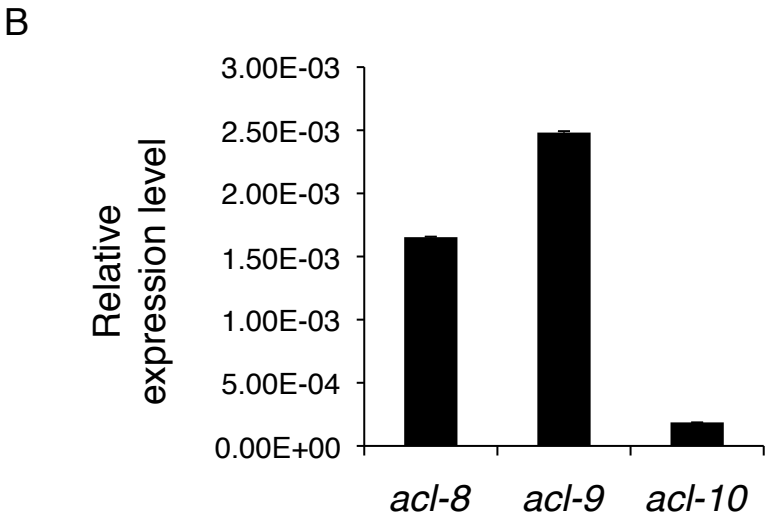

Supplementary Figure 11. (A) Negative ionization LC/ESI-MS spectra of PI molecular species of wild-type (upper) and *acl-10* mutants (lower). 'a' refers to alkyl ether linkage. (B) Quantitative RT-PCR analysis of *acl-8*, *acl-9* and *acl-10* expression. Expression of *acl-8*, *acl-9* and *acl-10* was normalized to that of *act-1*.

Supplementary Figure 12

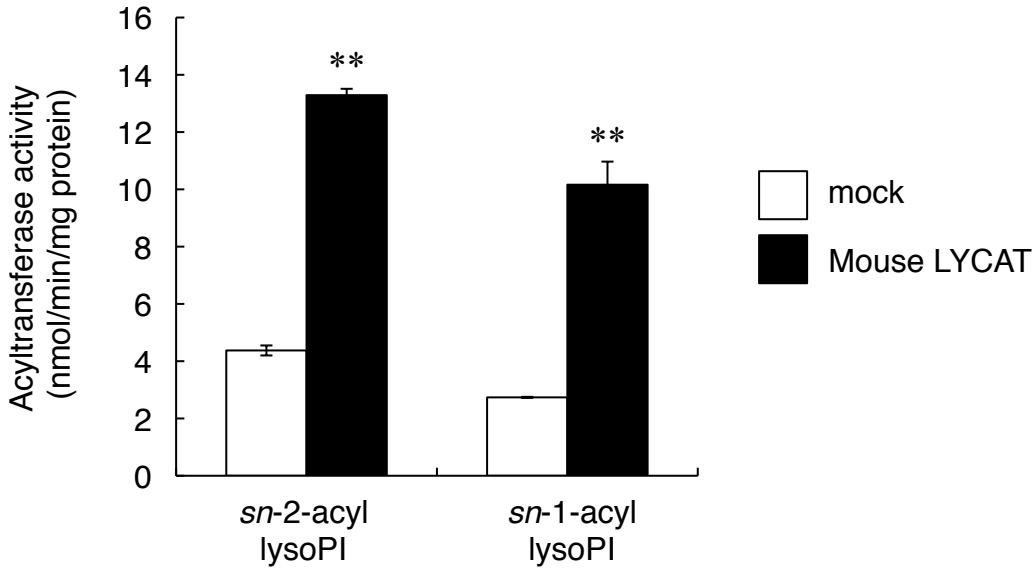

Supplementary Figure 12. Mouse LYCAT transfers stearic acid to the *sn*-1 position of PI as well as the *sn*-2 position of PI. HEK 293 cells were transfected with the mouse LYCAT expression plasmid. Expression of mouse LYCAT increased the LPIAT activities towards both *sn*-2-acyl lysoPI and *sn*-1-acyl lysoPI as acyl acceptors. [^{14}C]stearoy-CoA was used as an acyl donor. Each bar represents the mean ± SEM of at least three independent experiments. ***P*<0.01.

References

Beigneux, A. *et al*. (2006). Agpat6--a novel lipid biosynthetic gene required for triacylglycerol production in mammary epithelium. J. Lipid Res. 47, 734-744.

Lewin, T., Wang, P., and Coleman, R. (1999). Analysis of amino acid motifs diagnostic for the sn-glycerol-3-phosphate acyltransferase reaction. Biochemistry 38, 5764-5771.